Desalination and Water Treatment
www.deswater.com
doi: 10.5004/dwt.2023.29613

298 (2023) 53–60
June

Bio-mediated synthesis of Cu-TiO_2 nanoparticles using *Phoenix dactylifera* lignocellulose as capping and reducing agent for the catalytic degradation of toxic dyes

Faiza Hassan[a], Aqeel Abbas[a], Faisal Ali[a], Arif Nazir[a,*], Maryam Al Huwayz[b], Norah Alwadai[b], Munawar Iqbal[c,a], Zahid Ali[d,a]

[a]*Department of Chemistry, The University of Lahore, Lahore, Pakistan, emails: arif.nazir@chem.uol.edu.pk (A. Nazir), faiza.hassan@chem.uol.edu.pk (F. Hassan), aqeelsahotra33@gmail.com (A. Abbas), faisal.ali@chem.uol.edu.pk (F. Ali)*
[b]*Department of Physics, College of Sciences, Princess Nourah bint Abdulrahman University, P.O. Box: 84428, Riyadh 11671, Saudi Arabia, emails: mmalhuwyz@pnu.edu.sa (M. Al Huwayz), nmalwadai@pnu.edu.sa (N. Alwadai)*
[c]*Department of Chemistry, Division of Science and Technology, University of Education Lahore, Pakistan, email: bosalvee@yahoo.com*
[d]*State key Laboratory of Organic-Inorganic Composites, Beijing University of Chemical and Technology, Beijing 100029, China, email: zahidchemist521@gmail.com*

Received 7 February 2023; Accepted 26 May 2023

ABSTRACT

This research is focused on synthesis of Cu-TiO_2 nanoparticles (NPs) by bio-mediated method using *Phoenix dactylifera* fruit extract. The lignocellulosic entities of *P. dactylifera* fruit extract used as reducing and capping agent due to presence of higher contents of phenolics and flavonoids. These synthesized NPs are characterized by ultraviolet-visible spectroscopy (UV-Vis), Fourier-transform infrared spectroscopy, X-ray diffraction and scanning electron microscopy. Cu-TiO_2 NPs synthesized by bio-mediated method are cost effective and environmental friendly. Results showed the average size of NPs was found to be 32.07 nm. Furthermore, these NPs act as very effective and suitable nano-catalyst for dyes degradation and reduces the concentration of Rhodamine-B to 89.8% and methyl orange to 95.3% dyes in wastewater. Results revealed that the synthesized NPs could possibly be employed for degradation of other toxic pollutants particularly dyes.

Keywords: Biosynthesis; Cu-TiO_2; Nanocatalyst; Dye degradation; Environmental remediation

1. Introduction

Natural biomolecules are crucial in the development of nanoscale materials with control over their forms and sizes. By lowering the amount of toxic/hazardous moieties, the utilization of bio-based resources not only lowers the cost of synthesizing nanomaterials but also complies with the green chemistry principles [1–3].

Biosynthesized nanoparticles (NPs) outperform chemically synthesized NPs due to their generally smaller sizes, good stability, high surface area charge and superior photoluminescence emission properties for treatment of a variety of contaminants found in wastewater, such as dyes from synthetic wastewaters [4–7]. The advantages of using plant extracts as reductants and stabilizers to create magnetic nanoparticles (MNPs) are affordability, environmental friendliness, sustainability, and simplicity of usage. Additionally, compared to their counterparts made by the conventional method, the MNPs produced through synthetic means are nontoxic, more stable and uniform in size. Hence, bio-mediated preparation techniques have elevated to the forefront of MNPs synthesis research [8–12]. NPs have efficient

* Corresponding author.

catalytic properties in dye degradation and water treatment because of their large surface area, a crucial factor for catalysis. Homogeneous catalysis is exceedingly productive and selective, but it has limited temperature stability and removal of catalyst from the reaction medium is challenging. In contrast heterogeneous catalysts, unlike homogeneous catalysts, have the advantage of being able to be used at elevated temperatures and easily restored, but lacking a clear understanding of low selectivity and mechanical aspects, both of which are important for parameter improvement [13–15]. Transition metal NPs are important in catalysis because they mimic metal surface activation and catalysis on nanoscale, leading to efficiency and selection in heterogeneous catalysis [16,17]. Semiconductor oxides such as SnO_2, TiO_2, and ZnO have been studied extensively as photocatalysts.

Cu, like many other NPs, has remarkable activity in a variety of applications from materials to medical. Cu has garnered greater attention in organic synthesis due to its ease of availability, low cost, and ecologically favorable nature. Over the past few decades, many catalytic systems have been developed that provide the best choice for catalytic organic reactions from different types of copper, including the Suzuki reaction [18], the click reaction [19] and the oxygen acylation reaction [20–22].

Copper-based catalysts have been shown to be effective in the oxidation of methylene blue in many research papers. Under modest circumstances, a 99% activity was produced within 45 min of the reaction. Despite the benefits and potential of Cu-NPs (Cu-NPs) as a catalyst, Cu-NP catalysis has received less attention than that of other transition metals. Because of its peerless properties (physical, chemical and biological) Ag metal has been used in a variety of fields and has been incorporated into a wide range of consumer goods [23,24].

Water purification utilizing TiO_2 as a photo catalyst has gotten a lot of interest. The separation of the catalyst is a technical constraint of employing TiO_2 in powder form. TiO_2 micro-crystallites have discovered to be stably adhered to glass plates without deactivation. As an illustration, carbofuran mineralization was investigated. According to the findings, complete mineralization can be attained after irradiation for 15 h. This approach is inexpensive, and the plates can be reused without being deactivated. The demand for UV irradiation for water purification is the biggest disadvantage [25,26].

Due to its chemical structural stability, biocompatibility, physical, optical, and electrical properties, titanium dioxide (TiO_2) or titania is a well-known and well-researched material [21]. Anatase, rutile, brookite, and titanium are the four mineral forms. The crystalline structure of anatase type TiO_2 corresponds to the tetragonal system under UV irradiation, it is primarily utilized as a photocatalyst. Tetragonal crystal structure is also found in rutile TiO_2 (with prismatic habit). Titania is mostly used as a white pigment in water color. The crystal structure of brookite type TiO_2 is orthorhombic. TiO_2 is a relatively new monoclinic mineral [27,28]. The main objective of this study was to synthesize Cu-TiO_2 NPs using *P. dactylifera* lignocellulose as capping and reducing agent for the catalytic degradation of cationic dyes. The synthesized particles were investigated using UV-Visible, scanning electron microscopy (SEM), X-ray diffraction (XRD) and energy-dispersive X-ray spectroscopy (EDX). The potential was analyzed against the degradation of toxic dyes.

2. Materials and methods

2.1. Chemical required

The chemicals required for the synthesis of copper decorated titania (TiO_2/Cu-NPs) included titanium dioxide (TiO_2) (>97%) (Merck, Germany), copper sulfate pentahydrates ($CuSO_4{\cdot}5H_2O$) (>99%) (Sigma-Aldrich, UK), *Phoenix dactylifera* fruit extract (local market), distilled water (as aqueous media) and ethanol (Sigma-Aldrich, Germany).

2.2. P. dactylifera (dates) fruit extract

In the first step, *P. dactylifera* (dates) was purchased from local market and washed with distilled water to remove soil particles then cut into small pieces. Then 250 g of *P. dactylifera* (dates) used without seeds was and blend it for 15 min in 250 mL distilled water. The prepared extract was filtered and stored in refrigerator for further use.

2.3. Formation of NPs

First of all, prepared solutions of respective salts, that is, 0.04 M TiO_2 solution in ethanol prepared by dissolving 0.32 g TiO_2 in 100 mL ethanol. 0.2 M copper sulfate pentahydrates ($CuSO_4{\cdot}5H_2O$) solution is prepared by dissolving 5 g copper sulfate pentahydrates ($CuSO_4{\cdot}5H_2O$) in 100 mL.

Take 50 mL of each solutions and mix them for half an hour with magnetic stirrer. after that add 50 mL dates extract and start heating and stirring for 1 h slowly. The reaction was observed critically and temperature was maintained at 40°C. Cu-TiO_2 NPs were first identified when the color of reaction changed (Fig. 1) from milky blue to milky green in 15 min after the continuous stirring of 1 h, the solution was set aside and left for 24 h to settled down the particles.

2.4. Separation and purification

Solutions was filtered and NPs were collected on filter paper. These NPs were shifted to evaporating dish and dried at room temperature. After drying, the synthesized material was stored in Eppendorf tubes. The liquid sample was stored in glass vials (Fig. 2):

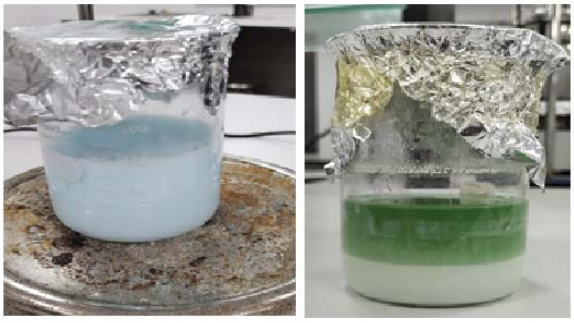

Fig. 1. Reaction progress shown from initial to final change.

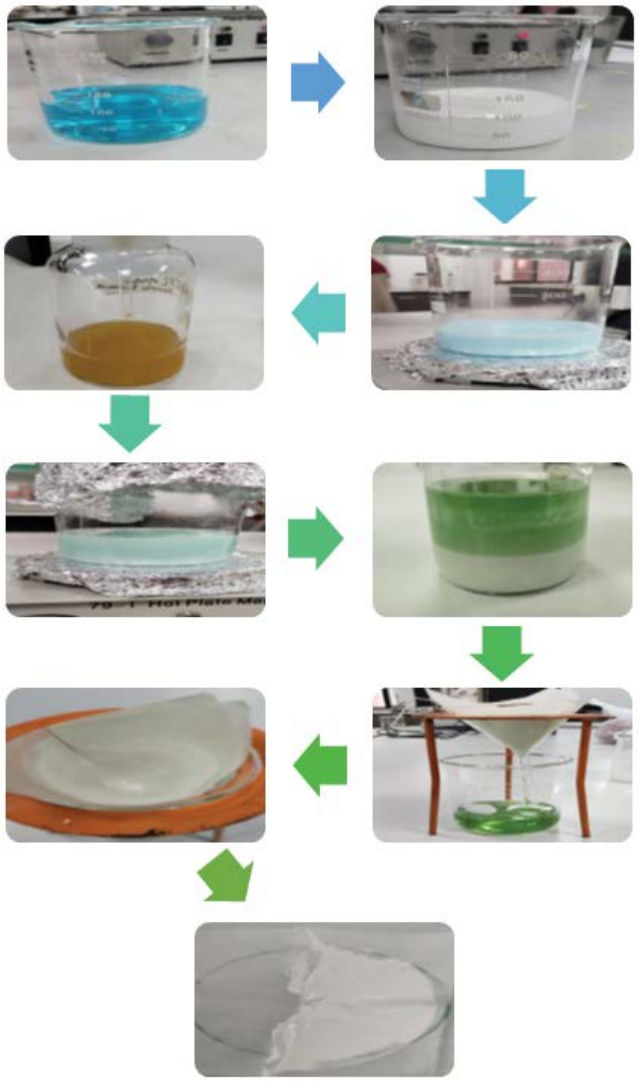

Fig. 2. Schematic flow sheet diagram for the synthesis of Cu-TiO_2 NPs.

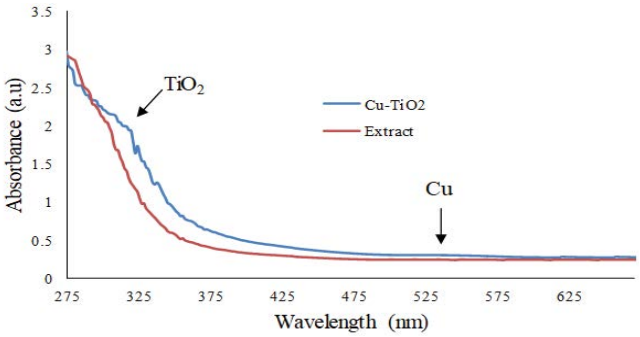

Fig. 3. UV-Visible spectrum of Cu-TiO_2 NPs.

2.5. Characterization

Different types of spectroscopies are applied to characterize the prepared NPs. Matter interaction with radiations leads to radiation rerouting and energy level changes. When a lower to higher level transition occurs during absorption, energy is transferred from the radiation field to the atom/molecule [29]. The preliminary determination of TiO_2/Cu-NPs stabilized using *P. dactylifera* was done over UV-Vis spectrophotometer (Cecil Aquarius CE 7400S, UK). The functional groups involved in nanocomposite were confirmed using FTIR (Bruker Alpha II, UK). Furthermore, the nano sized morphology and EDX were examined using SEM (NOVA FESEM-450, UK). In the last, the crystalline studies were monitored over XRD (Bruker D8 having 1.54 Å λ with Cu Kα).

2.6. Catalytic degradation of Rhodamine-B and methyl orange

The catalytic degradation of Rhodamine-B (Rh-B) was done suing the following conditions 1.8 mL of 0.027 mM Rh-B, 21.3 mg/mL nanocomposite and 0.7 mL of 9.6 mM $NaBH_4$. While, methyl orange (MO) dye was catalytically degraded using 1.3 mL of 0.058 mM MO dye, 21.3 mg/mL nanocomposite and 0.6 mL of 12.5 mM $NaBH_4$. The degradation of cationic dyes using $NaBH_4$ on the nanocomposite surface was performed over UV-Vis spectrophotometer.

3. Results and discussion

3.1. UV-Vis analysis

UV-Visible spectroscopy was employed to characterize the NPs. Fig. 3 shows the UV-Visible absorption spectra of the produced Cu-TiO_2 NPs. Full scan of sample was done. The scan of *P. dactylifera* fruit extract which was used as reference showed no peak while we can see a clear peak of Cu-NPs at 547 nm and slight peak of TiO_2 at 327 nm. In already reported data Cu-NPs show absorption in 520–600 nm [30]. TiO_2 show strong absorption peak between 200 and 380 nm [31].

3.2. Functional group analysis

The Fourier-transform infrared (FTIR) spectra of Cu-TiO_2 NPs grown in *P. dactylifera* fruit extract are shown in Fig. 4. According to the peaks of Cu-TiO_2 NPs had broad wavenumber range of 650–1,000 cm^{-1}. Date seeds, like the fruit flesh, are rich in phytochemicals such as flavonoids, polyphenols, phytosterols and carotenoids thus making them potential candidates for deriving extracts capable of synthesizing NPs [32]. The peaks at 3,258 and 1,627 cm^{-1} are associated with O–H stretch bend, respectively. Ti–O–Ti bond showed a dip for stretching vibration in the range of 400–800 cm^{-1} in the given sample of NPs due to definite absorbance in this range. In contrast with the un-doped TiO_2, the doped TiO_2 displayed supplementary absorbance peaks at 1,471; 1,252 and 1,082 cm^{-1}. Cu–O exhibited band below 1,000 cm^{-1} associated with vibrations. These outcomes established the doping of N and Cu species into the TiO_2 lattice [33].

3.3. Crystallinity of synthesized NPs

X-ray diffraction analysis determines crystallographic structure of the synthesized NPs. It involves bombardment of incoming X-rays on NPs and then measure the

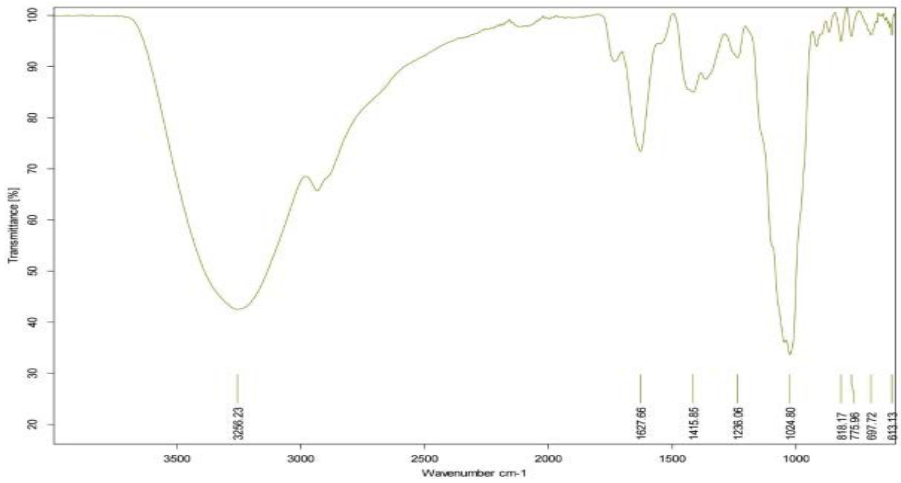

Fig. 4. Functional group illustration of Cu-TiO_2 NPs.

intensity and scattering angles of the X-rays that escape. After few days of synthesis, the XRD pattern

Cu-TiO_2 reveals seven wide peaks at 2θ = 19.88, 28.15, 36.78, 41.85, 55.04, 57.22, 69.84 shows miller indices (006), (110), (420), (520), (700), (640), (830), respectively. This shows that Cu-TiO_2 have cubic crystal lattice in their crystal structure (Fig. 5). Average crystal size is 0.2918 nm [34].

3.4. Morphology of NPs

The SEM images taken at different resolution clearly shown the particles are very fine. Agglomeration and aggregation takes place during the particle growth process. Fig. 6 displays the morphology of prepared Cu-TiO_2 NPs as determined by SEM. It was observed that the fabricated nanoparticles have spherical morphology and furthermore, the doping has no effect on morphological appearance except the slight agglomeration. However, at high dopant concentration, grain size increases as indicated by agglomeration [35].

3.5. Degradation analysis

3.5.1. Rhodamine-B

Rh-B is a dye of the xanthene class, red in color, which is soluble in water. Rh-B, commonly known as water tracer fluorescent, is widely used as a coloring additive in the food and textile sectors. Rh-B is poisonous and effects the eyes, skin, and respiratory tract if consumed by animals or humans. Apart from dyes, the widespread use of antibiotics, as well as their buildup and resistance against degradability in the environment, cause global domain issues [36].

It is reported that Rh-B dye (aqueous solution) absorbs visible light between the wavelengths of 460 and 600 nm. Maximum peak of absorption in the visible band were observed at 554 nm in aqueous Rh-B solution. Cu-TiO_2, TiO_2-SiO_2, and Cu-TiO_2-SiO_2 nanocomposites were tested for their photocatalytic activity for the breakdown of Rh-B in aqueous solution under both UV (11 W) and visible (500 W halogen lamp and low-pressure mercury bulb,

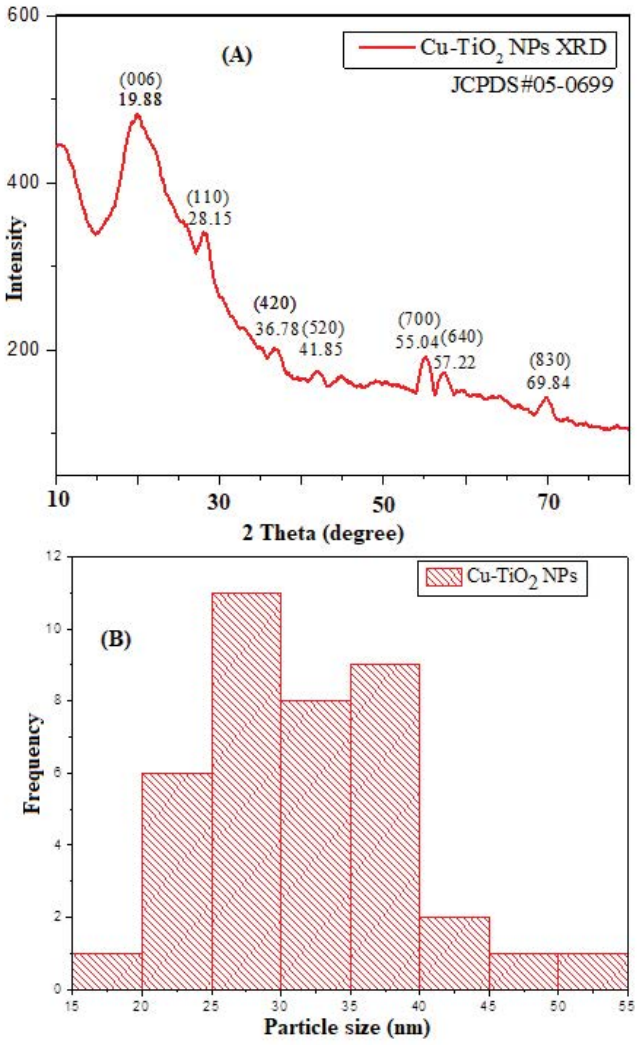

Fig. 5. (A) X-ray diffraction spectra showing the nature of crystallinity of Cu-TiO_2 NPs (B) Average particle size of bio-mediated synthesized bimetallic NPs.

respectively, lamp) light irradiation. A specific quantity of the 25 mL solution received the appropriate photocatalysts. A beaker full of Rhodamine-B (5 mg/L). The stoppage was swirled in the dark for 30 min to achieve the adsorption–desorption balance. UV and visible lamp is then used. the suspension was turned on, the solution samples were taken out of the reactor on a regular basis and the catalyst powder was separated using centrifugation. The resultant filtrate's absorbance was observed at 552 nm by UV-Vis spectrophotometer. The graphs show that the absorption is maximum at 560 nm and it decreases gradually with the passage of time. The Cu-TiO_2 act as a catalyst as it lower concentration of dye [37].

$NaBH_4$ converted the azo dyes into their hydrazine derivatives while, the cationic dye Rh-B were converted to Leuco Rh-B (Fig. 7). However, these dyes are not

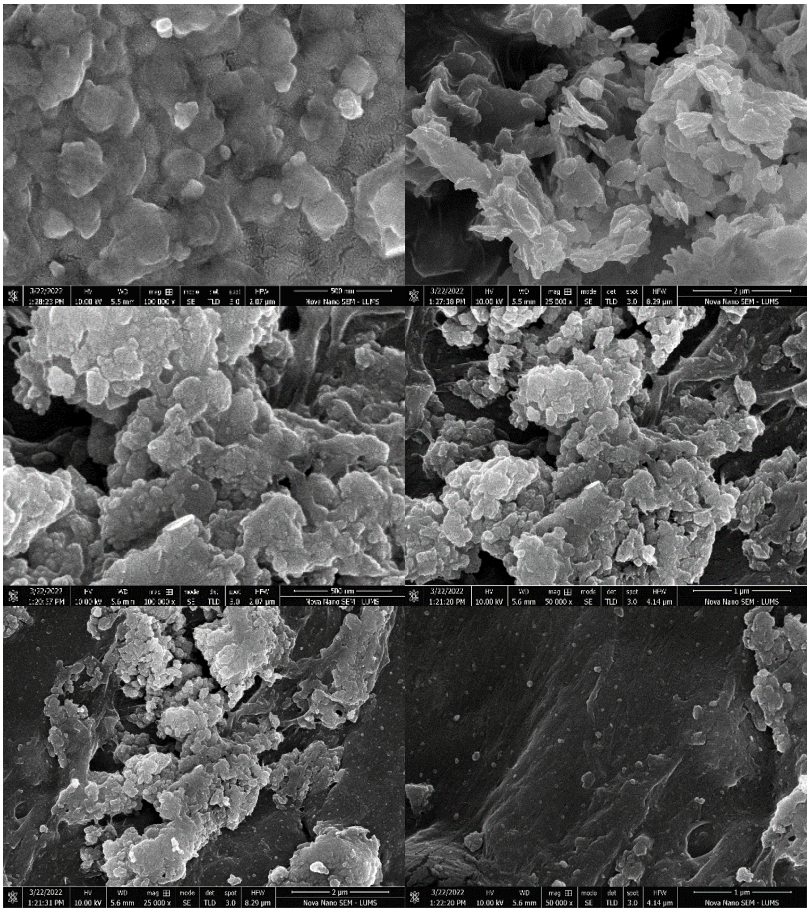

Fig. 6. Scanning electron microscopy images of Cu-TiO_2 exhibiting the morphology of particles.

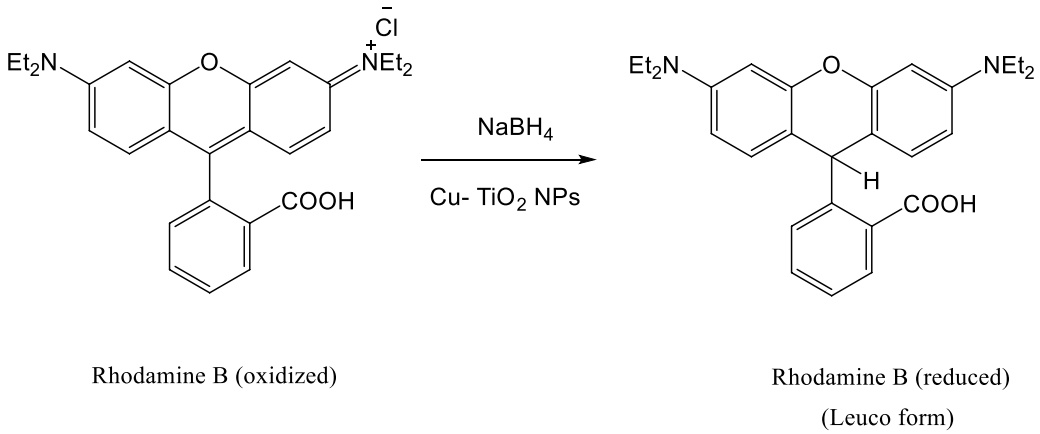

Rhodamine B (oxidized)

Rhodamine B (reduced)
(Leuco form)

Fig. 7. Reduction of Rhodamine-B dye in the presence of reducing agent and synthesized NPs.

completely reduced even by the excess amount of borohydride. Both catalyst and borohydride are needed for this reaction. Both catalyst and borohydride are needed for this reaction. The kinetics were applied on the degradation studies which was 0.25 min^{-1} having % degradation value 89.8% (Fig. 8). This nano-catalyst shows the maximum degradation among all the previously reported catalysts against Rh-B dye (Table 1).

3.5.2. Methyl orange

A negative-charged dye is known as an anionic dye. The azo dye family includes methyl orange (MO). MO is commonly used as an indication in different industries for fabrics, plastic and paper, cosmetics, medicines and drugs, rubber, dye processing, and printing establishments. It is a serious environmental hazard because of its limited degradability because of the reactivity of an azo group. Diarrhea, vomiting, nausea, and trouble breathing are all possible side effects of methyl orange. Methyl orange is also used as an indicator for weak acid–base with carcinogenic and toxic properties. As a result, MO must be removed from the aquatic environment and eradicated. In aqueous solution, MO shows high and small absorption peak at 467. We employed $NaBH_4$ to minimize methyl orange using Cu-TiO_2 nanoparticle as catalyst in this experiment as the time passes the absorbance decreases which shows that dye is degraded. It is degraded in 25 min (Figs. 9 and 10). The MO degradation gives the kinetics values from Fig. 10b, which was –0.1363 min^{-1}. The % degradation of MO using Cu-TiO_2 nano-catalyst was highest among all earlier reported data 95.30% Fig. 10c, Table 2.

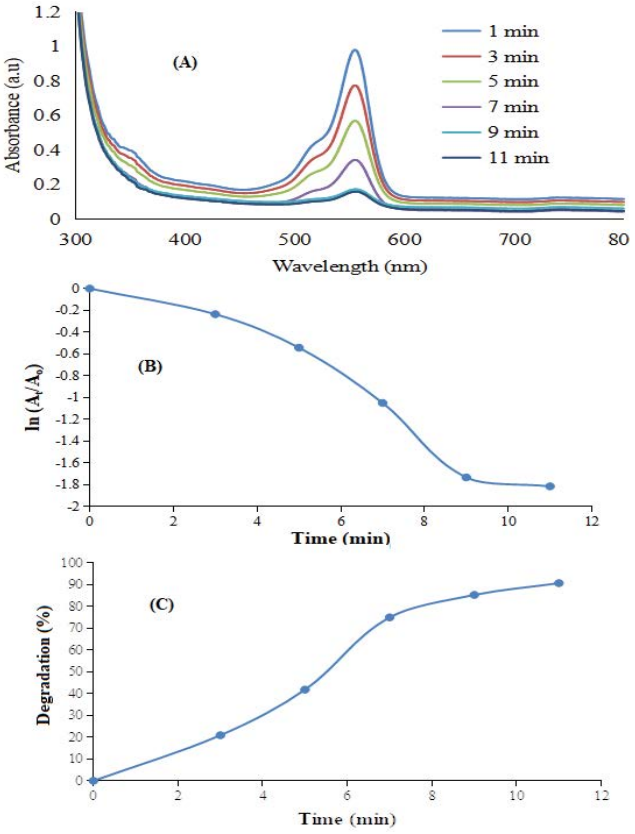

Fig. 8. Degradation of Rhodamine-B (A) optimized conditions (conc. 0.027 mM, nanocatalyst 21.3 mg/mL and $NaBH_4$ 9.6 mM and (B) kinetics of Rhodamine-B dye and (C) dye degradation (%) with reference to time.

Table 1
Literature showing the comparison of Rhodamine-B dye degradation in different reported studies

S. No.	Supporting material	Metal nanoparticle	Degradation (%)	Reaction time (min)	Method	References
1	Hollow carbon sphere	TiO_2, TiO_2 HS, Cu_2O/TiO_2, Cu_2O/TiO_2 heterostructured hollow spheres	Cu_2O/TiO_2 HS 87%	120–300	Photocatalyst	[21]
2	Carbon black-cellulose acetate sheets	Ag-Cu-ZnO/cellulose	88	14	Catalysis	[21]
4	Kaolinite clay	Cu-TiO_2	26	180	Photocatalyst	[22]
5	Kaolinite clay	Cu-TiO_2	52–69	180	Visible light	[22]
6	*Phoenix dactylifera*	Cu-TiO_2	89.8%	11	Catalysis	This work

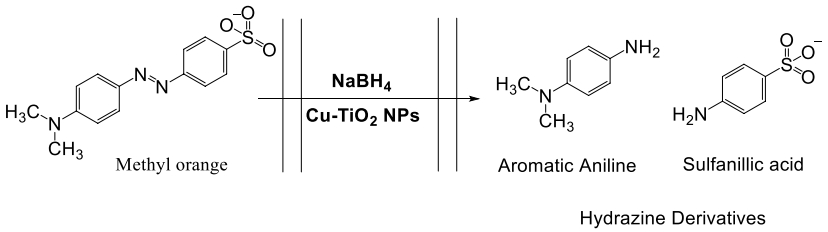

Fig. 9. Reduction of methyl orange dye in the presence of reducing agent and synthesized NPs.

Table 2
Literature review for methyl orange degradation studies

S. No.	Supporting material	Metal nanoparticle	Degradation (%)	Reaction time (min)	Method	Ref.
1	Carbon black-cellulose acetate sheets	Ag-Cu-ZnO/cellulose	88	12	Catalysis	[20]
2	Chitosan	Ni-Al	92.00 Cu, N Co doped TiO_2 > $NTiO_2$ > Cu-TiO_2 > TiO_2	360	Adsorption	[26]
3	Gelatin	Cu-TiO_2/ZnO NPs	83.00 (3% Cu-TiO_2/30% ZnO) > 61.00 (3% Cu-TiO_2)	60	Photocatalytic	[27]
4	Ripened *Duranta erecta* fruits	Cu-NPs	96	4	Catalysis	[28]
5	*Phoenix dactylifera*	Cu-TiO_2 NPs	95.3%	25	Catalysis	This work

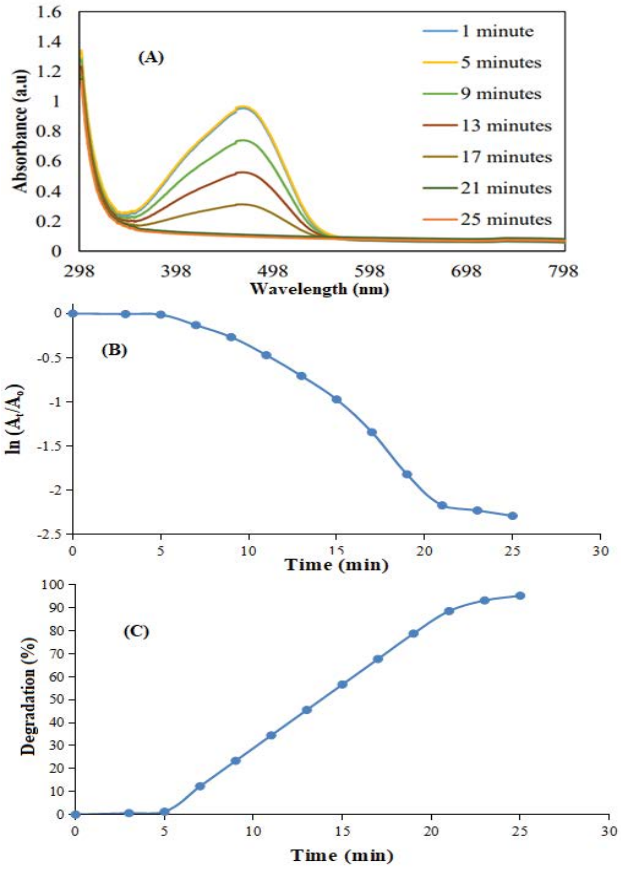

Fig. 10. Degradation of methyl orange dye (A) optimized conditions (conc. 0.058 mM, catalyst 21.3 mg/mL and $NaBH_4$ 12.5 mM, (B) kinetics of methyl orange degradation and (C) dye degradation (%) vs time.

4. Conclusions

We have synthesized Cu-TiO_2 NPs by bio-mediated eco-friendly and cost effective method. For this purpose, *P. dactylifera* fruit extract was used as a stabilizing agent due to its high content of phenolics and flavonoids. These NPs were characterized by FTIR, UV-Visible, XRD and SEM. The UV-Visible spectrum of sample showed peak of Cu at 547 nm and TiO_2 at 327 nm. FTIR studies have shown the characteristic functionalities for the synthesized material. XRD analysis indicates cubic shape of crystals. SEM revealed the morphology of NPs with fine agglomeration and aggregation takes place during the particle growth process. After that the catalytic activity of these Cu-TiO_2 NPs was analyzed against cationic dyes. They are proved very effective in the presence of $NaBH_4$ against the reduction of Rh-B in just 11 min with remarkable efficiency of 90% and reduction of MO in only 25 min with 95.3% efficacy. Rhodamine-B was degraded comparatively in a more effective way. This probably conclude that the prepared material could be effective against toxins particularly dyes.

Funding

This research was funded by Princess Nourah bint Abdulrahman University Researchers Supporting Project number (PNURSP2023R439), Princess Nourah bint Abdulrahman University, Riyadh, Saudi Arabia

Acknowledgments

The authors express their gratitude to Princess Nourah bint Abdulrahman University Researchers Supporting Project number (PNURSP2023R439), Princess Nourah bint Abdulrahman University, Riyadh, Saudi Arabia.

References

[1] R.S. Dhabbe, S. Sabale, T.T. Salunkhe, M.M. Vadiyar, A.N. Kadam, 3 - Biogenic Synthesis of Metal Oxide-Based photocatalysts for Dye Removal, S.P. Govindwar, M.B. Kurade, B.-H. Jeon, A. Pandey, Eds., Current Developments in Bioengineering and Biotechnology, Elsevier, Amsterdam, Netherlands, 2023, pp. 69–109.
[2] V.V. Gawade, S.R. Sabale, R.S. Dhabbe, K.M. Garadkar, Environmentally sustainable synthesis of SnO_2 nanostructures for efficient photodegradation of industrial dyes, J. Mater. Sci.: Mater. Electron., 34 (2023) 138, doi: 10.1007/s10854-022-09455-4.
[3] R.J. Kamble, P.V. Gaikwad, K.M. Garadkar, S.R. Sabale, V.R. Puri, S.S. Mahajan, Photocatalytic degradation of malachite green using hydrothermally synthesized cobalt-doped TiO_2 nanoparticles, J. Iran. Chem. Soc., 19 (2022) 303–312.
[4] A.K. Saim, P.C.O. Adu, R.K. Amankwah, M.N. Oppong, F.K. Darteh, A.W. Mamudu, Review of catalytic activities of

biosynthesized metallic nanoparticles in wastewater treatment, Environ. Technol. Rev., 10 (2021) 111–130.
[5] E. David, Evaluation of behavior of 13X zeolite modified with transition metals for catalytic applications, Bioinorg. Chem. Appl., 2022 (2022) 7352074, doi: 10.1155/2022/7352074.
[6] C.P. Ukpaka, O.N. Neo, Modeling of *Azadirachta indica* leaves powder efficiency for the remediation of soil contaminated with crude oil, Chem. Int., 7 (2021) 62–70.
[7] M.W. Shammout, A.M. Awwad, A novel route for the synthesis of copper oxide nanoparticles using *Bougainvillea* plant flowers extract and antifungal activity evaluation, Chem. Int., 7 (2021) 71–78.
[8] H.N. Bhatti, S. Sadaf, M. Naz, M. Iqbal, Y. Safa, H. Ain, S. Nawaz, A. Nazir, Enhanced adsorption of Foron Black RD 3GRN dye onto sugarcane bagasse biomass and Na-alginate composite, Desal. Water Treat., 216 (2021) 423–435.
[9] R.A. Khera, M. Iqbal, A. Ahmad, S.M. Hassan, A. Nazir, A. Kausar, H.S. Kusuma, J. Niasr, N. Masood, U. Younas, R. Nawaz, M.I. Khan, Kinetics and equilibrium studies of copper, zinc, and nickel ions adsorptive removal on to *Archontophoenix alexandrae*: conditions optimization by RSM, Desal. Water Treat., 201 (2020) 289–300.
[10] D.N. Iqbal, H. Yousaf, N. Masood, M. Iqbal, A. Nazir, Factors affecting the efficiency of rye husk as a potential biosorbent for the removal of metallic pollutants from aqueous solutions, Desal. Water Treat., 206 (2020) 74–82.
[11] A. Shokri, Employing electro coagulation for the removal of Acid Red 182 in aqueous environment using Box–Behenken design method, Desal. Water Treat., 115 (2018) 281–287.
[12] A. Shokri, Investigation of UV/H_2O_2 process for removal of ortho-toluidine from industrial wastewater by response surface methodology based on the central composite design, Desal. Water Treat., 58 (2017) 258–266.
[13] S.K. Jha, A. Jha, Plant extract mediated synthesis of metal nanoparticles, their characterization and applications: a green approach, Curr. Green Chem., 8 (2021) 185–202.
[14] O. Wenjie, W. Ahmed, F. Xiuxian, W. Lu, L. Jiannan, Y. Jie, R.M.A. Asghar, M. Mahmood, J.M. Alatalo, M. Imtiaz, W. Li, S. Mehmood, The adsorption potential of Cr from water by ZnO nanoparticles synthesized by *Azolla pinnata*, Bioinorg. Chem. Appl., 2022 (2022) 6209013, doi: 10.1155/2022/6209013.
[15] A.Y. Elderdery, B. Alzahrani, A.A. Alabdulsalam, S.M.A. Hamza, A.M.E. Elkhalifa, A.H. Alhamidi, F. Alanazi, A. Mohamedain, S.K. Subbiah, P. Ling Mok, Structural, optical, antibacterial, and anticancer properties of cerium oxide nanoparticles prepared by green synthesis using *Morinda citrifolia* leaves extract, Bioinorg. Chem. Appl., 2022 (2022) 6835625, doi: 10.1155/2022/6835625.
[16] C. Altinkaynak, E. Kocazorbaz, N. Özdemir, F. Zihnioglu, Egg white hybrid nanoflower (EW-hNF) with biomimetic polyphenol oxidase reactivity: synthesis, characterization and potential use in decolorization of synthetic dyes, Int. J. Biol. Macromol., 109 (2018) 205–211.
[17] A.M. Awwad, M.W. Amer, M.M. Al-Aqarbeh, TiO_2-kaolinite nanocomposite prepared from the Jordanian kaolin clay: adsorption and thermodynamics of Pb(II) and Cd(II) ions in aqueous solution, Chem. Int., 6 (2020) 168–178.
[18] M.B. Thathagar, J. Beckers, G. Rothenberg, Copper-catalyzed Suzuki cross-coupling using mixed nanocluster catalysts, J. Am. Chem. Soc., 124 (2002) 11858–11859.
[19] B.H. Lipshutz, B.R. Taft, Heterogeneous copper-in-charcoal-catalyzed click chemistry, Angew. Chem. Int. Ed., 45 (2006) 8235–8238.
[20] S. Jammi, S. Sakthivel, L. Rout, T. Mukherjee, S. Mandal, R. Mitra, P. Saha, T. Punniyamurthy, CuO nanoparticles catalyzed C–N, C–O, and C–S cross-coupling reactions: scope and mechanism, J. Org. Chem., 74 (2009) 1971–1976.
[21] A. Nazir, M. Raza, M. Abbas, S. Abbas, A. Ali, Z. Ali, U. Younas, S.H. Al-Mijalli, M. Iqbal, Microwave assisted green synthesis of ZnO nanoparticles using *Rumex dentatus* leaf extract: photocatalytic and antibacterial potential evaluation, Z. Phys. Chem., 236 (2022) 1203–1217.
[22] N. Khaliq, I. Bibi, F. Majid, M.I. Arshad, A. Ghafoor, Z. Nazeer, S. Ezzine, N. Alwadai, A. Nazir, M. Iqbal, $Mg_{1-x}Ni_xFe_{2-x}Cr_xO_4$ synthesis via hydrothermal route: effect of doping on the structural, optical, electrical, magnetic and photocatalytic properties, Results Phys., 43 (2022) 106059, doi: 10.1016/j.rinp.2022.106059.
[23] A. Nazir, S. Farooq, M. Abbas, E.A. Alabbad, H. Albalawi, N. Alwadai, A.H. Almuqrin, M. Iqbal, Synthesis, characterization and photocatalytic application of *Sophora mollis* leaf extract mediated silver nanoparticles, Z. Phys. Chem., 235 (2021) 1589–1607.
[24] A. Jamil, T.H. Bokhari, T. Javed, R. Mustafa, M. Sajid, S. Noreen, M. Zuber, A. Nazir, M. Iqbal, M.I. Jilani, Photocatalytic degradation of disperse dye Violet-26 using TiO_2 and ZnO nanomaterials and process variable optimization, J. Mater. Res. Technol., 9 (2020) 1119–1128.
[25] A. Nazir, A. Akbar, H.B. Baghdadi, S. ur Rehman, E. Al-Abbad, M. Fatima, M. Iqbal, N. Tamam, N. Alwadai, M. Abbas, Zinc oxide nanoparticles fabrication using *Eriobotrya japonica* leaves extract: photocatalytic performance and antibacterial activity evaluation, Arabian J. Chem., 14 (2021) 103251, doi: 10.1016/j.arabjc.2021.103251.
[26] S. Ali, M. Iqbal, A. Naseer, M. Yaseen, I. Bibi, A. Nazir, M.I. Khan, N. Tamam, N. Alwadai, M. Rizwan, M. Abbas, State of the art of gold (Au) nanoparticles synthesis via green routes and applications: a review, Environ. Nanotechnol. Monit. Manage., 16 (2021) 100511, doi: 10.1016/j.enmm.2021.100511.
[27] A. Nazir, M.I. Sharafat Hussain, N. Ahmad, Phytochemical remediation and detoxification of aflatoxins in cattle feed, Chem. Int., 8 (2022) 153–158.
[28] S.M. Gajare, M.V. Patil, R.T. Mahajan, Phytochemical screening and antimicrobial activity of ethanol extract of *Calotropis procera* root, Int. J. Res. Phytochem. Pharmacol., 2 (2012) 143-146.
[29] M.D.A. Sanda, M. Badu, J.A.M. Awudza, N.O. Boadi, Development of TiO_2-based dye-sensitized solar cells using natural dyes extracted from some plant-based materials, Chem. Int., 7 (2021) 9–20.
[30] K. Ben Jeddou, F. Bouaziz, F. Ben Taheur, O. Nouri-Ellouz, R. Ellouz-Ghorbel, S. Ellouz-Chaabouni, Adsorptive removal of Direct Red 80 and methylene blue from aqueous solution by potato peels: a comparison of anionic and cationic dyes, Water Sci. Technol., 83 (2021) 1384–1398.
[31] R. Nankya, K.-N. Kim, Sol–gel synthesis and characterization of Cu-TiO_2 nanoparticles with enhanced optical and photocatalytic properties, J. Nanosci. Nanotechnol., 16 (2016) 11631–11634.
[32] M.N. Zafar, Q. Dar, F. Nawaz, M.N. Zafar, M. Iqbal, M.F. Nazar, Effective adsorptive removal of azo dyes over spherical ZnO nanoparticles, J. Mater. Res. Technol., 8 (2019) 713–725.
[33] Y. Slimani, M.A. Almessiere, A.D. Korkmaz, S. Guner, H. Güngüneş, M. Sertkol, A. Manikandan, A. Yildiz, S. Akhtar, S.E. Shirsath, $Ni_{0.4}Cu_{0.2}Zn_{0.4}Tb_xFe_{2-x}O_4$ nanospinel ferrites: ultrasonic synthesis and physical properties, Ultrason. Sonochem., 59 (2019) 104757, doi: 10.1016/j.ultsonch.2019.104757.
[34] Y. Yulizar, J. Gunlazuardi, D.O.B. Apriandanu, T.W.W. Syahfitri, CuO-modified $CoTiO_3$ via *Catharanthus roseus* extract: a novel nanocomposite with high photocatalytic activity, Mater. Lett., 277 (2020) 128349, doi: 10.1016/j.matlet.2020.128349.
[35] A. Lassoued, J.F. Li, Magnetic and photocatalytic properties of Ni–Co ferrites, Solid State Sci., 104 (2020) 106199, doi: 10.1016/j.solidstatesciences.2020.106199.
[36] F. Torki, H. Faghihian, Photocatalytic activity of NiS, NiO and coupled NiS–NiO for degradation of pharmaceutical pollutant cephalexin under visible light, RSC Adv., 7 (2017) 54651–54661.
[37] S. Sankar, S.K. Sharma, N. An, H. Lee, D.Y. Kim, Y.B. Im, Y.D. Cho, R.S. Ganesh, S. Ponnusamy, P. Raji, Photocatalytic properties of Mn-doped NiO spherical nanoparticles synthesized from sol-gel method, Optik, 127 (2016) 10727–10734.